

Detection Limits for Electron Energy-Loss Spectroscopy in Biology

Richard D. Leapman* and S. Brian Andrews**

*Division of Bioengineering and Physical Science, ORS; **Laboratory of Neurobiology, NINDS, National Institutes of Health, Bethesda, MD 20892

Advances in electron energy loss spectroscopy (EELS), both in the scanning transmission electron microscope (STEM) and the energy-filtering transmission electron microscope (EFTEM), have created new opportunities for biological microanalysis. In particular, more sensitive detectors have improved detection limits [1-5], and spectrum-imaging software for acquiring EELS data pixel by pixel has increased flexibility for mapping the distributions of biologically important elements [6-9].

Under optimum conditions, EELS offers higher sensitivity than electron-probe x-ray microanalysis, although the two techniques are generally complementary. For example, EELS can be used to measure concentrations of calcium within membrane-bound cellular compartments [11], or to determine the distributions of phosphorus contained in phosphorylated proteins and nucleic acid - protein complexes [12-14]. Spectrum-imaging in the EFTEM provides an alternative quantitative approach for mapping elements that occur at relatively high concentrations over larger specimen areas, e.g., to map covalently bound sulfur in proteins [15]. Although the characteristic core-edge signal is high in EELS, so is the underlying background, which gives rise to small signal-to-background ratios [16]. For example, phosphorus and sulfur typically occur at atomic fractions of 0.01 or lower, and calcium concentrations can be lower than 10 atomic parts per million (~1 mmol/kg). In favorable preparations single atom detection is feasible for core-loss elemental maps acquired in a STEM equipped with a field-emission source. Thus, EELS can be applied to broad range of biological structures from the cellular to the supramolecular level.

Here, we illustrate some of the capabilities of EELS microanalysis provided by an efficient detector system and the Gatan Digital Micrograph spectrum-imaging software. Experiments were performed using a VG Microscopes HB501 STEM equipped with a Gatan Enfina 1000 spectrometer incorporating a cooled charge-coupled device (CCD) [2]. This detector has several advantages, including (i) fast read-out, (ii) square elements enabling accurate correction for channel gain variations, and (iii) low read-out noise.

The prediction of single-atom detectability has been tested by recording spectrum-images from hemoglobin molecules adsorbed onto a thin carbon film along with ferritin molecules as a reference standard (Fig. 1). Results show that the four heme groups in a single molecule are detected with a signal-to-noise ratio of ~10:1. Other measurements demonstrate that calcium adsorbed onto a thin carbon film can be imaged at single atom sensitivity with a signal-to-noise ratio of ~5:1. A comparison of theoretical and experimental signal-to-noise ratios for detecting single atoms of Fe and Ca is shown in Fig. 2 [10]. Despite radiation damage due to the necessarily high electron dose, it is anticipated that mapping single atoms of metals and other bound elements will find useful applications in characterizing large protein assemblies.

References

- [1] Z. Tang et al., *J. Microsc.* 175 (1994) 100.
- [2] J.A. Hunt et al., *Microsc. Microanal.* 7 (suppl. 2) (2001) 1132.
- [3] H. Brink et al., *Microsc. Microanal.* 6 (Suppl. 2) (2000) 212.
- [4] A.J. Gubbens et al., *Ultramicroscopy* 51 (1993) 146.
- [5] O.L. Krivanek et al., *Ultramicroscopy*. 59 (1995) 267.
- [6] C. Jeanguillaume and C. Colliex, *Ultramicroscopy* 28 (1989) 252.

- [7] J.A. Hunt and D.B. Williams, *Ultramicroscopy* 38 (1991) 47.
 [8] J.A. Hunt and R.H. Harmon, *Microsc. Microanal.* 4 (Suppl. 2) (1998) 152.
 [9] R.D. Leapman and N.W. Rizzo, *Ultramicroscopy* 78 (1999) 251.
 [10] R.D. Leapman, *J. Microsc.* (2003) in press.
 [11] R.D. Leapman et al., *Ultramicroscopy* 49 (1993) 225.
 [12] D.P. Bazett-Jones et al., *Science* 264 (1994) 1134.
 [13] F.P. Ottensmeyer, *J. Ultrastruct. Res.* 88 (1984) 121.
 [14] R.D. Leapman et al., *Proc. Natl. Acad. Sci. USA* 94 (1997) 7820.
 [15] G. Goping et al., *Microsc. Res. Tech* (2003) in press.
 [16] H. Shuman and P. Kruit, *Rev. Sci. Instrum.* 56 (1985) 231.

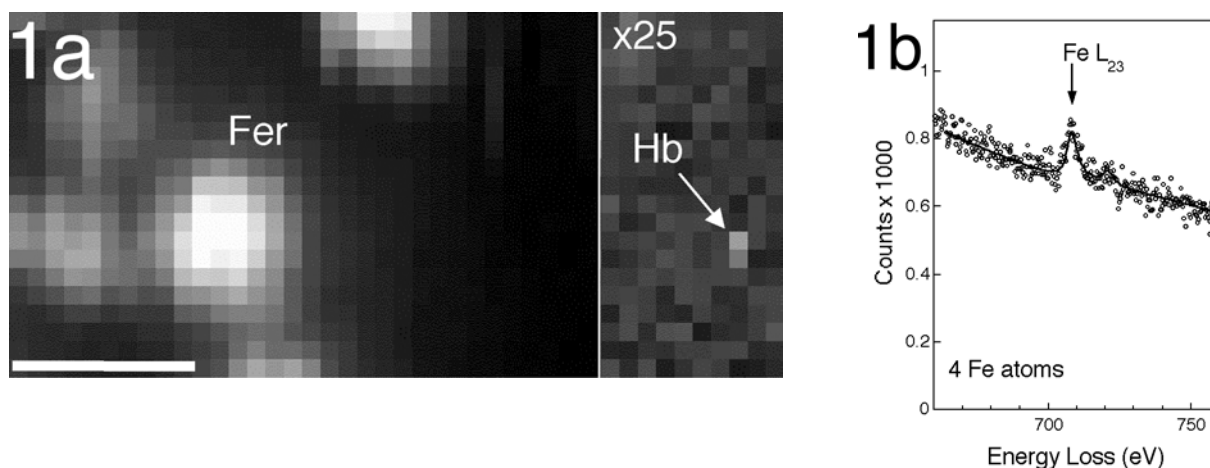


FIG. 1. (a) Iron distribution of ferritin and hemoglobin molecules supported on a thin 4 nm carbon film obtained by STEM-EELS using spectrum-imaging at the Fe $L_{2,3}$ edge. On the left of image, a filled ferritin core is present, containing around 4000 Fe atoms. After increasing the intensity scale by a factor of 25 on the right of image, a two-pixel feature is visible (arrow), attributed to a single hemoglobin molecule containing four Fe atoms. Bar = 10 nm. (b) EELS extracted from spectrum-image for the feature indicated by arrow in Fig. 1, with least-squares fit to Fe $L_{2,3}$ edge reference spectrum from ferritin core, showing signal-to-noise ratio of $\sim 10:1$. The integrated intensity ratio of ferritin core to hemoglobin has the expected value of $\sim 1000:1$.

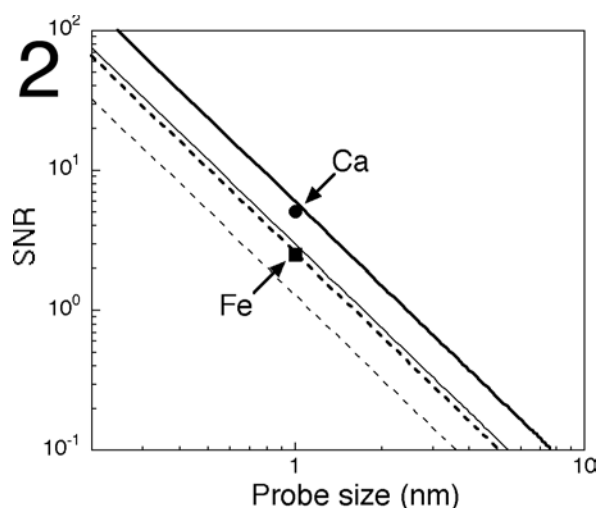


FIG. 2. Calculated signal-to-noise ratio for detecting single atoms of Ca and Fe supported on a thin 4 nm carbon film, as a function of probe size. Predicted values are displayed on a logarithmic plot for a total incident electron charge of 0.1 nC (Ca, thin solid line; Fe, thin dashed line) and for an incident charge of 0.4 nC (Ca, thick solid line; Fe, thick dashed line). Experimental measurements are included for a 0.4 nC incident electron charge into a 1 nm probe size (Ca, circle; Fe square).